Quantitative Analysis of Dynamic Gd-DTPA Enhancement in Breast Tumors Using a Permeability Model

Paul S. Tofts, Bruce Berkowitz, Mitchell D. Schnall

The MRI signal enhancement in a breast tumor, measured as a function of time after a bolus injection of Gd-DTPA, may contain enough information to differentiate malignant from benign tissue. We find a physiological model for measuring capillary permeability and leakage space (P. S. Tofts, A. G. Kermode, measurement of the blood-brain barrier permeability and leakage space using dynamic MR imaging. 1. Fundamental concepts. *Magn. Reson. Med.* 17, 357–367 (1991)) fits the data well. The enhancement curve is particularly sensitive to the preinjection T_1 of the tumor, the dose, and the time of injection. This model may provide a means of characterizing the pathophysiology of breast tumors from the Gd-DTPA enhancement curve.

Key words: breast; MRI; Gd-DTPA; tumor.

INTRODUCTION

There is increasing interest in characterizing breast tumors from their dynamic signal enhancement curves, measured using a T_1-weighted sequence (usually a spoilt gradient echo sequence) after injection of a bolus of Gd-DTPA (1–7). However, publications from different laboratories have conflicted over how the enhancement curve data should be interpreted. Quantitative characterization of the enhancement curves requires a complete appreciation of the underlying physiological and MR physics mechanisms involved in the generation of the enhancement curve. We explore the applicability of the model of Tofts and Kermode for Gd-DTPA signal enhancement (8), first developed for blood-brain barrier lesions studied with T_1-weighted spin echo images, but theoretically relevant to any tissue with leaking capillaries (including tumor tissue). This model has been applied to blood-retina barrier leakage, where the permeability values have been validated by a physiological technique (9) and has been simplified for rapid measurements of low permeability lesions (10). Infusion injection protocols have been shown to be less efficient than bolus injections (11). Larsson *et al.* produced a similar model (12), although the analysis method was different. This was shown to produce similar values of permeability and leakage space (13). A summary of this note has been presented previously (14).

MRM 33:564–568 (1995)

From the NMR Research Group, Institute of Neurology, National Hospital for Neurology and Neurosurgery, London, United Kingdom (P.S.T.); the Department of Ophthalmology and Radiology, University of Texas Southwestern Medical Center, Dallas, Texas (B.B); and the Department of Radiology, University of Pennsylvania Medical Center, Philadelphia, Pennsylvania (M.S.)

Address correspondence to: Paul Tofts, D. Phil., Institute of Neurology, Queen Square, London WC1N 3BG, United Kingdom.

Received July 27, 1994; revised November 21, 1994; accepted November 22, 1994.

0740-3194/95 3.00

THEORY

According to the model of Tofts and Kermode (8), after injection of a bolus dose D mmole/kg body weight, given at time $t = 0$, the plasma concentration decays biexponentially. In humans, the data of Weinmann *et al.* (15) have been fitted (8) to give amplitudes $a_1 = 3.99$ kg/liter, $a_2 = 4.78$ kg/liter, and rate constants $m_1 = 0.144$ min^{-1}, $m_2 = 0.0111$ min^{-1}. The resulting tissue concentration is (8)

$$C_t(t) = D\,k\sum_{i=1}^{2} a_i(e^{-m_3t} - e^{-m_it})/(m_i - m_3) \qquad [1]$$

where k is the permeability surface area product/unit volume of tissue (referred to as "permeability" for convenience), v_l is the leakage space, i.e., the proportion of the leaky tissue into which Gd-DTPA can leak ($0 < v_l < 1$), and $m_3 = k/v_l$. The relaxivities in tissue are assumed to be equal to those in aqueous solution ($R_1 = 4.5$ s^{-1} mM^{-1}, $R_2 = 5.5$ s^{-1} mM^{-1} at 21°C and 1.5 T) (16). The signal from a spoilt gradient echo sequence is (17)

$$S(C_t) = G\,PD e^{-TE(T_{20}^{*-1} + R_2C_t)} \sin(\theta)\,\frac{1 - e^{-TR(T_{10}^{-1} + R_1C_t)}}{1 - cos(\theta)e^{-TR(T_{10}^{-1} + R_1C_t)}} \qquad [2]$$

where G is the gain, PD is the proton density, and T_{20}^*, T_{10} are the values of T_2^* and T_1 before injection of Gd-DTPA. The signal enhancement is

$$E(t) = \frac{S(C_t) - S(0)}{S(0)} \qquad [3]$$

where $S(0)$ is the signal in the absence of Gd-DTPA ($C_t = 0$). Using Eqs. [1] and [2], this can be expressed as a function of the permeability k, the leakage space v_l; the plasma parameters a_1, a_2, m_1, and m_2; dose D; relaxivities R_1 and R_2; and T_{10}. The expression for E has no dependence on T_{20}*.

The recommended practical measurement procedure is as follows: T_{10} is measured, Gd-DTPA is injected as a bolus without moving the patient, and the signal is measured as a function of time, starting with a point before injection of Gd-DTPA and then continuously imaging as enhancement builds up. The enhancement is fitted using Eqs. [1–3], with k and v_l as the only free parameters. A convenient way of measuring T_{10} is to collect a proton

density-weighted (i.e., relaxed) image before the series of T_1-weighted images by increasing the *TR* or reducing the tip angle. The number of excitations can be increased for improved precision. T_{10} is then calculated from the pre-injection proton density-weighted and T_1-weighted images.

METHODS

A range of datasets (6) from patients with breast cancer were least squares fitted to the model. They had been collected using a dose of 0.1 mmole/kg and a spoilt gradient echo (SPGR) sequence on a General Electric 1.5 T Signa imager, with TR = 50 ms, TE = 6 ms, θ = 60°. Values of the T_1 of the tumor before injection of Gd-DTPA (T_{10}) were not available. A value for normal tissue of 710 ms (18) was assumed in order to demonstrate the model. Other T_{10} values were also used to investigate the sensitivity of the method to T_{10}. Several model enhancement curves were simulated at different values of T_{10} to demonstrate the influence of T_{10}.

The sensitivity of the fitted values of permeability k and leakage space v_l to errors in the assumed parameters (D, a_1, a_2, m_1, m_2, R_1, R_2, T_{10}, t, TR, TE, and θ) was found as follows: A representative dataset was taken (the medium permeability lesion shown in Fig. 1b). Each parameter in turn was reduced to 99% of its nominal value and the data refitted with the reduced parameter value. This simulates the effect of data produced when the true parameter value is 1% higher than expected. The fractional increase in fitted k and v_l was found and divided by 1% to give the error propagation ratio (EPR), defined as (fractional change in fitted k or v_l)/(fractional change in parameter).

RESULTS

The fits were good, with no apparent difference in the shapes of the measured enhancement curves and those produced by the model. Data for tumors with a range of permeabilities are shown in Fig. 1. The three lesions show distinctly different enhancement curves. The most slowly enhancing lesion (Fig. 1a) was still rising after 4 min; the more quickly enhancing lesion (Fig. 1b) reached a plateau; the most quickly enhancing lesion started to decrease within 4 min. Estimated values for permeability k were in the range 0.1–1.2 min^{-1}, and estimates of v_l varied from 0.3–0.8.

Altering the T_{10} value (i.e., the assumed value of tumor T_1 in the absence of Gd-DTPA) had a dramatic effect on the fitted values (Table 1). The goodness of fit was not affected and therefore cannot be used to estimate the correct T_{10}. There was a factor of 2.8 between the highest and lowest T_{10} values, and these produced permeability values varying by a factor of 3.4 and leakage space values varying by a factor of 4.0.

The influence of T_{10} on enhancement is dramatically shown in Fig. 2, where the simulated enhancement curves for a single tumor (k = 0.5 min^{-1}, v_l = 0.7) are plotted for a range of T_{10} values. For T_{10} = 710 ms, a 10%

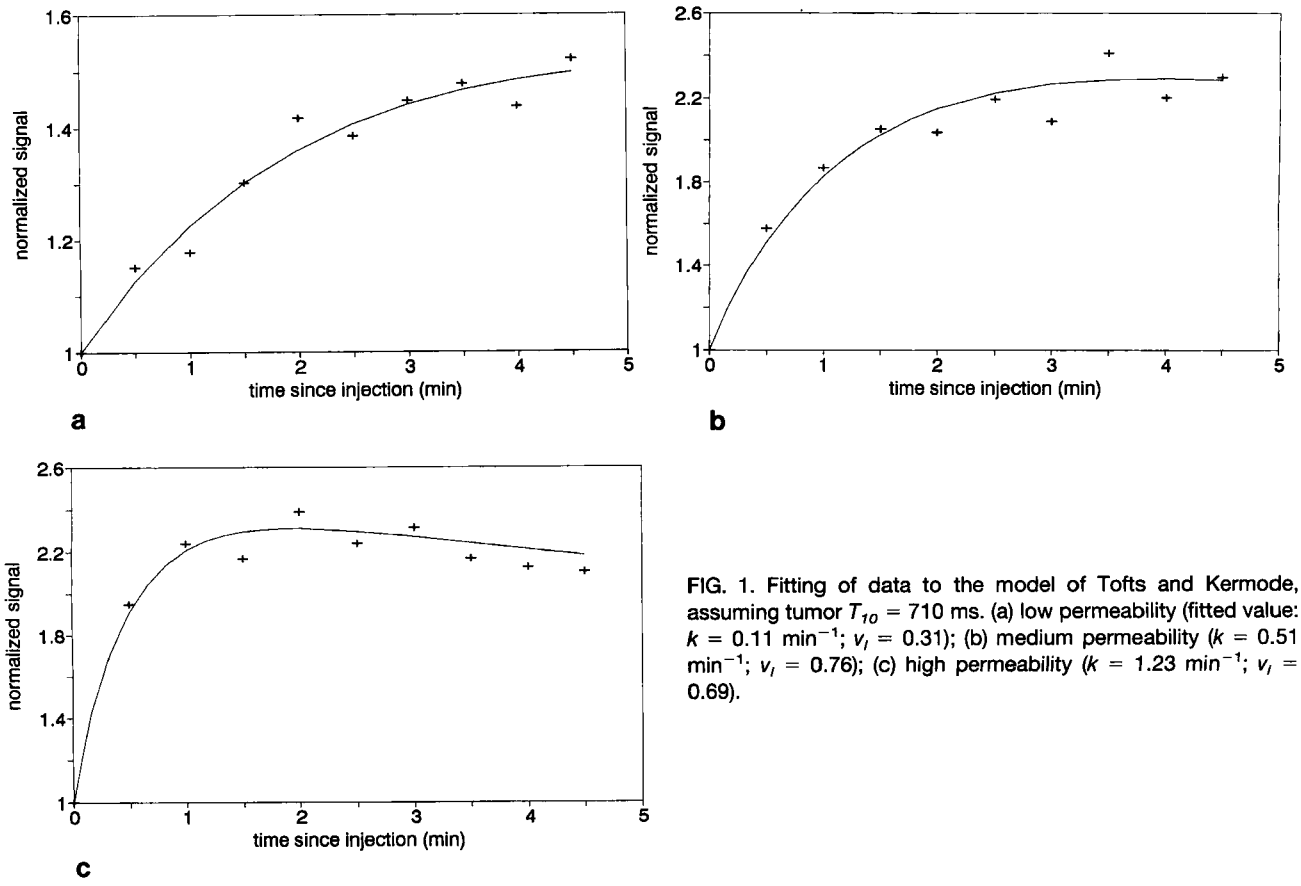

FIG. 1. Fitting of data to the model of Tofts and Kermode, assuming tumor T_{10} = 710 ms. (a) low permeability (fitted value: k = 0.11 min^{-1}; v_l = 0.31); (b) medium permeability (k = 0.51 min^{-1}; v_l = 0.76); (c) high permeability (k = 1.23 min^{-1}; v_l = 0.69).

Table 1
Effects of the Assumed Tumor T_1 Value (T_{10}) on Fitted Values of Permeability k and Leakage Space v_l, for the Medium Permeability Data Shown in Fig. 1b (Measured at 1.5 T)

Tissue	T_{10} (s)	k (min^{-1})	v_l	RMS residual error in fit
Normal low risk fatty portion (18)	0.46	0.88	1.43	0.091
Tumor - low T_1 (20)	0.60	0.63	0.96	0.092
Normal high risk diffuse density portion (18)	0.71	0.51	0.76	0.093
Tumor - high T_1 (20)	1.3	0.26	0.36	0.095

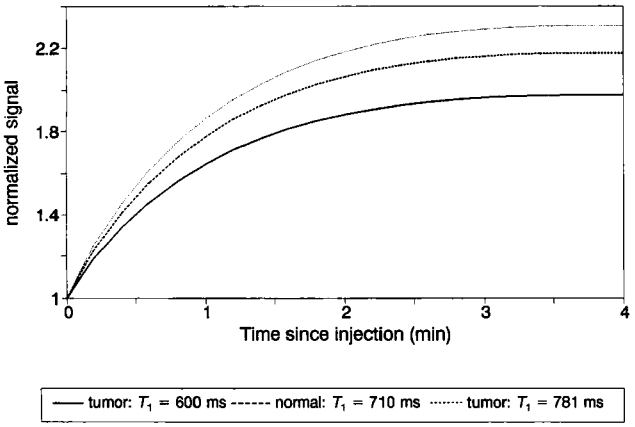

FIG. 2. The effect of tumor T_1 (*i.e.*, T_{10}) on the Gd-DTPA enhancement curve for a simulated medium permeability tumor (k = 0.5 min^{-1}; v_l = 0.7). The lowest and highest tumor T_1 values (600 and 1300 ms (20) are shown, with normal high risk diffuse density tissue (T_1 = 710 ms (18)).

increase in T_{10} gives an 11% increase in enhancement at all times after injection. (The enhancement is the proportional change in signal relative to that before enhancement, i.e., the normalized signal minus 1).

Several parameters had high EPRs, with absolute values of at least 1.0 (see Table 2). These are the dose (D), the T_1 relaxivity (R_1), the tumor T_1 (T_{10}), and the time after injection (t).

DISCUSSION

The accuracy with which a breast tumor can be characterized using this approach is limited by how accurately parameters listed in Table 2 can be determined; the EPR values give quantitative guidance on which parameters are most critical. The dose should be carefully measured, ideally to an accuracy of 1%. The R_1 relaxivity is intrinsic to the tumor and cannot be measured directly. Published *in vivo* values show very little change from the *in vitro* value (19). Any alterations that are present will reflect alterations in tumor pathology. Because an alteration in R_1 will always affect the enhancement curve (i.e., the signal versus time curve), almost any analysis of the curve is susceptible to errors from R_1 changes. However, the shape of the enhancement curve is independent of R_1 (provided the signal is linearly proportional to the

Table 2
Propagation of Errors in Assumed Parameter Values to Estimate of Permeability k and Leakage Space v_l[a]

Parameter		Nominal value	EPR[b]	
			k	v_l
Dose	D	0.1 mmole/kg	1.0	1.0
Plasma curve amplitudes	a_1	3.99 kg liter^{-1}	0.5	0.3
	a_2	4.78 kg liter^{-1}	0.5	0.7
Plasma curve	m_1	0.144 min^{-1}	0.04	−0.2
Decay rates	m_2	0.0111 min^{-1}	0.01	−0.03
T_1 relaxivity	R_1	4.5 s^{-1} mM^{-1}	1.0	1.0
T_2 relaxivity	R_2	5.5 s^{-1} mM^{-1}	−0.02	−0.04
T_1 of tumor	T_{10}	710 ms	1.2	1.3
Time after injection	t	100 s	2.1	−0.6
Repetition time	TR	50 ms	−0.2	−0.3
Echo time	TE	6 ms	−0.02	−0.04
Tip angle	θ	60°	0.4	0.7

[a] For medium permeability tumor (k = 0.5 min^{-1}; v_l = 0.7) as shown in Fig. 1.
[b] The EPR is defined as (fractional change in fitted k or v_l)/(fractional change in parameter). For example, if the true value of T_{10} were 10% higher than assumed for the fitting procedure, the estimated value of permeability k would be about 12% higher than the true value.
[c] A 1-s error in timing the center of the bolus injection (i.e., 1% error in t) would give a 2.1% error in k.

Gd-DTPA concentration), and k/v_l can be extracted from this without assuming an R_1 value (12, 13). This can also be seen from the EPR values (Table 1). An error in R_1 (or D) produces exactly the same fractional error in k as in v_l, and hence no change in k/v_l. The effect of T_{10} errors on k/v_l is also very small. The *in vivo* R_2 relaxivity could differ from the *in vitro* value; however, the dependence of enhancement on R_2 is weak, because a short TE is used (EPR = −0.04 in Table 1).

The T_1 of the tumor in the absence of Gd-DTPA (i.e., T_{10}) may have a wide range of values. In normal tissue it varies from 460 ms in the low risk fatty portion to 710 ms in the higher risk diffuse density portion (18), and in tumors it can range from 600-1300 ms (20). The precise value makes a large difference to the enhancement curve and must be taken into account in the analysis of the curve, whatever model is used. T_{10} should be measured as accurately as possible, and this may be the most limiting step in characterizing the tumor. Under good conditions, in the brain, it can be measured with an accuracy of 2% (21); if this were possible in the breast, it would give an inaccuracy of 2.4% in the permeability (using the EPR of 1.2; see Table 2). A quality assurance program may be needed to ensure that the T_{10} values are accurate and stable and that the spoilt gradient echo sequence in use does indeed have the dependence on T_1 given by Eq. [2].

The timing of the injection is crucial, and this may be the other limiting step in characterizing the tumor. Variations in the injection procedure can be minimized by keeping the injection rate constant during injection and by keeping the duration short (less than 30 s). Bolus injections of duration 4 s can be achieved without the use of power-assisted equipment (22). Timing should be from the center of the injection period and measured to within 1 s. Images should also be timed at the center, because this is when the low spatial frequencies that determine signal intensity are usually collected.

The model assumes that the bolus is instantly mixed into the plasma pool after injection. Although this must take some time, the high quality of the fits (Fig. 1) suggests that inaccuracies in the model related to mixing and passage of the bolus are minimal and will remain constant provided the injection protocol is not altered. The duration of the enhancement, peaking at least 2 min after injection, suggests that the amount of tracer that leaks from the capillaries during the first pass of the bolus is small, and therefore, any T_2*-mediated signal losses during that first pass can be ignored. The plasma curve may depart from those measured in normal subjects by Weinmann *et al.* (15); however, the effects of renal function are minimal at short times after injection (10) (this is seen by the low EPR for m_2, the renal clearance rate; Table 2). Alterations in hydration status would probably affect a_1, a_2, and m_1. In serial measurements on a single patient, any deviations from normal would probably be present at each examination, giving a constant systematic error. Some workers have taken blood samples during the examination (12); however, this is an inconvenient procedure. The Gd-DTPA concentration in the samples must be measured in some way, and it may be hard to ensure that the timing of the samples is accurate. Two proposed methods of measuring *in vivo* the Gd-DTPA concentration in blood have been published (23, 24); perhaps these methods could be used if large variations in the plasma concentration between patients were suspected.

The Heidelberg group (3, 25) have used 2-min infusion injections to characterize tumors; we believe that a bolus injection is more appropriate for two reasons. First, a bolus achieves any given enhancement faster than an infusion does, and it also achieves a higher peak enhancement than an infusion of the same amount of tracer (11). Second, a fast process such as a rapidly enhancing tumor with $k = 1.2\ \text{min}^{-1}$, reaching maximum enhancement about 2 min after a bolus injection, is better probed with a bolus (effectively a delta function) than with an infusion that effectively smooths out the transient response of the tumor.

Dynamic uptake of Gd-DTPA in brain tumors has been studied by several groups. Schmiedl *et al.* (26) estimated the blood-to-tissue transport coefficient in a rat glioma model, finding values in the range 1–10 ml/kg min. Gowland *et al.* (27) used an inversion recovery echoplanar sequence and found values for k in the range of 0.01–1.5 min^{-1}. Ostergaard *et al.* (28) used a fast field echo sequence (an unspoilt gradient echo). Uptake was slower than in the breast tumors we studied, reaching its maximum at 7–15 min. They extracted a parameter that is equal to k/v_l (13); two tumors had $k/v_l = 0.08$ and 0.10 min^{-1}. We expect that the analysis applied in this paper to breast tumors is equally applicable to brain tumors.

The Tofts and Kermode model assumes that the flow is great enough for the plasma concentration not to be depleted by leakage from the capillary, i.e., that the lesion is well perfused and $k \ll F$ (8), where F is the flow. For this reason, in high permeability lesions, perhaps k should be referred to as an "apparent permeability" rather than a true one, because it may contain a flow component. The pathological significance of the leakage space (defined as the space into which Gd-DTPA can leak from the capillaries) in the case of tumors is still unclear. It probably includes the extracellular space and may also include capillaries that are not well connected to the main blood supply. Animal experiments would probably clarify where the tracer is located. Electron microscopy would confirm the presence of Gd in particular locations by x-ray dispersive microanalysis. Alternatively, Fe-DTPA would have the same pharmacokinetics as Gd-DTPA and could be localized by staining and light microscopy.

In order to characterize breast tumors as fully as possible, there are at least two more parameters besides permeability and leakage space which should be considered. First, in any case, the T_1 of the tumor, T_{10}, must be measured and is "free" information that does not require any extra data collection time. Second, vascularity, or blood volume, has been estimated in the brain using bolus tracking in which T_2*-weighted images are collected every few seconds (22). The bolus passes through in about 20 s, so this information could be collected free before the conventional dynamic T_1-weighted enhancement curve. Thus, a total of four tissue-characterizing parameters obtained in a single examination may enable a better classification of tissue types by using clustering techniques (29) than would be available with only those derived from the enhancement curve.

We conclude that the permeability method discussed here is applicable to the analysis of signal enhancement in breast tumors. The two physiological parameters—permeability and leakage space—may enable breast tumors to be characterized, assist in distinguishing benign from malignant tumors, and stage and assess response to treatment. Some questions remain unanswered regarding the validity of the model and the correct values of parameters to be used in the estimation procedure. Nonetheless, it is the best model currently available and provides considerably more insight into the basic pathophysiology than does the simpler approach of merely measuring signal enhancement. The estimated physiological parameters are independent of the particular sequence used and provide a way of standardizing measurements from a variety of MRI sites. Studies that investigate the correlation between these parameters and the pathological status of tumors as determined from biopsies are now required.

REFERENCES

1. W. A. Kaiser, E. Zeitler, MR imaging of the breast: fast imaging sequences with and without Gd-DTPA. *Radiology* **170**, 681–686 (1989).
2. J. P. Stack, O. M. Redmond, M. B. Codd, P. A. Dervan, J. T. Ennis, Breast disease: tissue characterisation with Gd-DTPA enhancement profiles. *Radiology* **174**, 491–494 (1990).
3. G. Brix, W. Semmler, R. Port, L. R. Sehad, G. Layer, W. J. Lorenz, Pharmacokinetic parameters in CNS Gd-DTPA enhanced MR imaging. *J. Comput. Assist. Tomogr.* **15**, 621–628 (1991).
4. D. A. Turner, J. Z. Wang, S. G. Economou, Functional images from dynamic, contrast enhanced 3DFT MR images for the detection of breast cancer, *in* "Proc., SMRM, 12th Annual Meeting, New York, 1993," p. 116.
5. R. M. Weisskoff, C. A. Hulka, B. Smith, K. McCarthy, D. A. Hall, G. J. Whitman, D. B. Kopans, T. J. Brady, Dynamic

NMR imaging of the breast using echo planar imaging, *in* "Proc., SMRM, 12th Annual Meeting, New York, 1993," p. 119.
6. M. D. Schnall, S. Orel, L. Muenz, Analysis of time intensity curves for enhancing breast lesions, *in* "Proc., SMRM, 12th Annual Meeting, New York, 1993," p. 120.
7. F. Kelcz, G. E. Santyr, S. J. Mongin, E. J. Fairbanks, Reducing false positive Gadolinium-enhanced breast MRI results through parameter analysis of the enhancement profile, *in* "Proc., SMRM, 12th Annual Meeting, New York, 1993," p. 121.
8. P. S. Tofts, A. G. Kermode. Measurement of the blood-brain barrier permeability and leakage space using dynamic MR imaging. 1. Fundamental concepts. *Magn. Reson. Med.* **17,** 357–367 (1991).
9. B. A. Berkowitz, P. S. Tofts, H. A. Sen, N. Ando, E. de Juan, Accurate and precise measurement of blood-retinal barrier breakdown using dynamic Gd-DTPA MRI. *Invest. Ophthalmol. Visual Sci.* **33,** 3500–3506 (1992).
10. P. S. Tofts, B. A. Berkowitz, Rapid measurement of capillary permeability using the early part of the dynamic Gd-DTPA MRI enhancement curve. *J. Magn. Reson. part B* **102,** 129–136 (1993).
11. P. S. Tofts, B. Berkowitz, Measurement of capillary permeability from the Gd enhancement curve—a comparison of bolus and constant infusion injection methods. *Magn. Reson. Imaging* **12,** 81–91 (1994).
12. H. B. W. Larsson, M. Stubgaard, J. L. Frederiksen, M. Jensen, O. Henriksen, O. B. Paulson, Quantitation of blood-brain barrier defect by magnetic resonance imaging and Gadolinium-DTPA in patients with multiple sclerosis and brain tumors. *Magn. Reson. Med.* **16,** 117–131 (1990).
13. H. B. W. Larsson, P. S. Tofts, Measurement of blood brain barrier permeability using dynamic Gd-DTPA scanning—a comparison of methods. *Magn. Reson. Med.* **24,** 174–176 (1992).
14. P. S. Tofts, B. Berkowitz, M. Schnall, Quantitative characterisation of breast tumours using dynamic Gd-DTPA MR imaging, *in* "Proc., SMR, 2nd Meeting, San Francisco, 1994," p. 1461.
15. H. J. Weinmann, M. Laniado, W. Mutzel, Pharmacokinetics of GdDTPA/Dimeglumine after intravenous injection into healthy volunteers. *Physiol. Chem. Phys. Med. NMR* **16,** 167–172 (1984).
16. P. S. Tofts, B. Shuter, J. M. Pope, Ni-DTPA doped agarose gel—a phantom material for Gd-DTPA enhancement measurements. *Magn. Reson. Imaging* **11,** 125–133 (1993).
17. F. W. Wehrli, "Fast-Scan Magnetic Resonance," 1st ed., p. 12, Raven Press, New York, 1991.
18. C. S. Poon, M. J. Bronskill, R. M. Henkelman, N. F. Boyd, Quantitative magnetic resonance imaging parameters and their relationship to mammographic pattern. *J. Natl. Cancer Inst.* **84,** 777–781 (1992).
19. R. B. Lauffer, Paramagnetic metal complexes as water proton relaxation agents for NMR imaging: theory and design. *Chem. Rev.* **87,** 901–927 (1987).
20. P. A. Bottomley, C. J. Hardy, R. E. Argersinger, G. Allen-Moore, A review of ^{1}H nuclear magnetic resonance relaxation in pathology: are T_1 and T_2 diagnostic? *Med. Phys.* **14,** 1–37 (1987).
21. P. S. Tofts, E. P. G. H. DuBoulay, Towards quantitative measurements of relaxation times and other parameters in the brain. *Neuroradiology* **32,** 407–415 (1990).
22. R. R. Edelman, H. P. Mattle, D. J. Atkinson, T. Hill, J. P. Finn, C. Mayman, M. Ronthal, H. M. Hoogewoud, J. Kleefield, Cerebral blood flow: assessment with dynamic contrast enhanced T_2*-weighted MR imaging at 1.5T. *Radiology* **176,** 211 (1990).
23. L. Sondergaard, H. B. W. Larsson, M. Stubgaard, O. Henriksen, The arterial concentration of Gd-DTPA can be monitored non-invasively, *in* "Proc., SMRM, 11th Annual Meeting, Berlin, 1992," p. 1120.
24. N. J. Taylor, I. J. Rowland, S. F. Tanner, M. O. Leach, A rapid interleaved method for measuring signal intensity curves in both blood and tissue during contrast agent administration. *Magn. Reson. Med.* **30,** 744–749 (1993).
25. T. Hess, M. V. Knopp, G. Brix, V. Hoffman, H. Junkerman, H. J. Zabel, G. van Kaick, Pharmacokinetic mapping of breast lesions by dynamic Gd-DTPA enhanced MRI, *in* "Proc., SMRM, 12th Annual Meeting, New York, 1993," p. 117.
26. U. P. Schmiedl, J. Kenney, K. R. Maravilla, Kinetics of pathologic blood-brain-barrier permeability in an astrocytic glioma using contrast-enhanced MR. *AJNR* **13,** 5–14 (1992).
27. P. Gowland, P. Mansfield, P. Bullock, M. Stehling, B. Worthington, J. Firth, Dynamic studies of gadolinium uptake in brain tumors using inversion-recovery echo planar imaging. *Magn. Reson. Med.* **26,** 241–258 (1992).
28. L. Ostergaard, C. Andersen, F. Tagehoj, S. Donstrup, J. Astrup, Blood-brain-barrier defect measurement using Fast Field Echo MRI, *in* "Proc., SMRM, 12th Annual Meeting, New York, 1993," p. 1624.
29. A. Simmons, G. J. Barker, P. S. Tofts, S. R. Arridge, Improvements to dual-echo clustering of neuroanatomy in MRI, *in* "Proc., SMRM, 11th Annual Meeting, Berlin, 1992," p. 4202.